ISSN 1330–0016
CODEN FIZBE7

DYNAMICAL CORRELATION AMONG MEDIUM-ENERGY PROTONS IN "HOT" AND "COLD" EVENTS IN RELATIVISTIC HEAVY-ION COLLISIONS

DIPAK GHOSH, KRISHNADAS PURKAIT and RANJAN SENGUPTA

High Energy Physics Division, Department of Physics, Jadavpur University, Calcutta 700 032, India

Received 6 March 1996

Revised manuscript received 17 March 1997

UDC 539.172, 539.1.073.7

PACS 25.70.Pq, 25.75.+r

Two- and three-particle dynamical correlation among protons have been studied separately in "hot" and in "cold" classes of events in ^{12}C-AgBr interaction at 4.5 A GeV/c.

1. Introduction

Recent results of experiments on ultrarelativistic heavy-ion collisions emphasize the importance of studying the particle production in the target fragmentation region [1]. The slow target-associated particles are produced in ultrarelativistic heavy-ion interaction is a quantitative probe of the cascading processes in the spectator parts of the target nucleus [2]. In emulsion terminology, the black-track-producing particles are evaporated from the excited target remnant in a late stage of collision whereas the gray-track-producing particles (gray particles) are mainly protons knocked out of the target nucleus in the later stage of the collisions [3]. Many of the features of the black and gray tracks cannot be trivially explained, and they put severe constraints on the models. Especially the observed stability of the angular distributions, which seems to be independent of any variable, might be important. The gray tracks deserve proper investigation because they are strongly correlated to

the produced particles [4]. They are supposed to remember part of the history of the reaction as they leave the nucleus at the same time scale with the secondaries of the interaction [5]. Therefore, it is important to investigate the correlations among particles produced in the disintegration of the target nuclei (i.e. gray particles). In relativistic heavy-ion collision, the study of two- and many-particle correlations presents significant features of the nuclear interaction and is a potential source of information. These correlations can provide direct information about the late stage of the reaction when nuclear matter is highly excited and diffused [6]. The correlation which prevails at the early stage of interaction cannot be expected to survive in the final state due to the rigors of the initial violent dense stage. The late diffused and deconfined stage is still far from normal unexcited nuclear matter. One may note that two- and three-particle inclusive correlations have been studied extensively for relativistic particles in heavy-ion collisions [7].

In our earlier work with relativistic α-particles emitted as projectile fragments in ^{12}C-emulsion interaction at 4.5 A GeV/c [8], it was observed that the projectile fragmentation region is characterized by two effective temperatures, of 10 MeV and of 40 MeV. Two distinctly different classes of events exist, namely "hot" and "cold" events with different reaction mechanisms. Our previous work with such events in ^{12}C-AgBr interactions at 4.5 A GeV/c showed some interesting results. We have observed that the pion coherence zones are different for "hot" and "cold" events [9]. Our observation in studying the factorial moments of the medium-energy protons reveals an intermittent pattern in the case of the "cold" events, but the "hot" events show no such self-similarity property [10]. We have studied the two-particle correlation among shower particles in two-temperature events [11]. We have also studied the multiplicity correlation for pions and protons emitted in both forward and backward hemispheres and observed the two-temperature events [12]. In the present paper, we study the two-particle and three-particle correlation for "cold" and "hot" events by comparing the experimental two-particle or three-particle angular correlation data with the Monte-Carlo simulated values, assuming an independent emission.

2. Method of analysis

2.1. Two-particle correlation

We investigated the two-particle correlation by using the standard correlation function

$$C(z_1, z_2) = \frac{1}{\sigma_{in}} \frac{\mathrm{d}^2\sigma}{\mathrm{d}z_1 \mathrm{d}z_2} - \frac{1}{\sigma_{in}^2} \frac{\mathrm{d}\sigma}{\mathrm{d}z_1} \frac{\mathrm{d}\sigma}{\mathrm{d}z_2},$$

where σ_{in}^2, $\mathrm{d}\sigma/\mathrm{d}z$, and $\mathrm{d}^2\sigma/(\mathrm{d}z_1\mathrm{d}z_2)$ are the inelastic cross-section, and the single- and the two-particle distributions, respectively. The inclusive correlation function (normalized) is defined as

$$R(z_1, z_2) = \left(\frac{1}{\sigma_{in}} \frac{\mathrm{d}^2\sigma}{\mathrm{d}z_1 \mathrm{d}z_2} - \frac{1}{\sigma_{in}^2} \frac{\mathrm{d}\sigma}{\mathrm{d}z_1} \frac{\mathrm{d}\sigma}{\mathrm{d}z_2} \right) \left(\frac{1}{\sigma_{in}^2} \frac{\mathrm{d}\sigma}{\mathrm{d}z_1} \frac{\mathrm{d}\sigma}{\mathrm{d}z_2} \right)^{-1}.$$

For gray particles, with $z = \cos\theta$,

$$R(\cos\theta_1, \cos\theta_2) = \left(\frac{1}{\sigma_{in}}\frac{\mathrm{d}^2\sigma}{\mathrm{d}\cos\theta_1 \mathrm{d}\cos\theta_2} - \frac{1}{\sigma_{in}^2}\frac{\mathrm{d}\sigma}{\mathrm{d}\cos\theta_1}\frac{\mathrm{d}\sigma}{\mathrm{d}\cos\theta_2}\right)\left(\frac{1}{\sigma_{in}^2}\frac{\mathrm{d}\sigma}{\mathrm{d}\cos\theta_1}\frac{\mathrm{d}\sigma}{\mathrm{d}\cos\theta_2}\right)^{-1} = \frac{NN_2(\cos\theta_1, \cos\theta_2)}{N_1(\cos\theta_1)N_2(\cos\theta_2)} - 1, \quad (1)$$

where $N_1(\cos\theta)$ is the number of grey particles with $\cos\theta$ between $\cos\theta$ and $\cos\theta + \mathrm{d}(\cos\theta)$, $N_2(\cos\theta_1, \cos\theta_2)$ is the number of pairs of grey particles within the intervals $\cos\theta_1$ to $\cos\theta_1 + \mathrm{d}(\cos\theta_1)$ and $\cos\theta_2$ to $\cos\theta_2 + \mathrm{d}(\cos\theta_2)$, and N is the total number of inelastic interactions in the sample.

2.2. Three-particle correlation

The above equation was extended to three particles by Levin et al. [13]:

$$R(z_1, z_2, z_3) = \frac{\rho_3(z_1, z_2, z_3) + 2\rho_1(z_1)\rho_1(z_2)\rho_1(z_3)}{\rho_1(z_1)\rho_1(z_2)\rho_1(z_3)} - \frac{\rho_2(z_1, z_2)\rho_1(z_3) + \rho_2(z_2, z_3)\rho_1(z_1) + \rho_2(z_3, z_1)\rho_1(z_2)}{\rho_1(z_1)\rho_1(z_2)\rho_1(z_3)}.$$

The quantities $\rho_1(z) = (1/\sigma)(\mathrm{d}\sigma/\mathrm{d}z), \rho_2(z) = (1/\sigma)(\mathrm{d}^2\sigma/(\mathrm{d}z_1\mathrm{d}z_2))$ and $\rho_3(z) = (1/\sigma)(\mathrm{d}^3\sigma/(\mathrm{d}z_1\mathrm{d}z_2\mathrm{d}z_3))$ represent, respectively, one-, two-, and three-particle densities. With the exchange $z_i = \cos\theta_i, i = 1, 2, 3$, the equation takes the form

$$R(\cos\theta_1, \cos\theta_2, \cos\theta_3) = \left\{\frac{1}{N}N_3(\cos\theta_1, \cos\theta_2, \cos\theta_3) + 2\frac{1}{N^3}N_1(\cos\theta_1)N_1(\cos\theta_2)N_1(\cos\theta_3) - \frac{1}{N^2}N_2(\cos\theta_1, \cos\theta_2)N_1(\cos\theta_3) - \frac{1}{N^2}N_2(\cos\theta_2, \cos\theta_3)N_1(\cos\theta_1) - \frac{1}{N^2}N_2(\cos\theta_3, \cos\theta_1)N_1(\cos\theta_2)\right\}\left[\frac{1}{N^3}N_1(\cos\theta_1)N_1(\cos\theta_2)N_1(\cos\theta_3)\right]^{-1},$$

where $N_1(\cos\theta)$ and $N_2(\cos\theta_1, \cos\theta_2)$ are defined above, and $N_3(\cos\theta_1, \cos\theta_2, \cos\theta_3)$ is the number of triplets of grey particles between $\cos\theta_1$ and $\cos\theta_1 + \mathrm{d}(\cos\theta_1)$, $\cos\theta_2$ and $\cos\theta_2 + \mathrm{d}(\cos\theta_2)$, and $\cos\theta_3$ and $\cos\theta_3 + \mathrm{d}(\cos\theta_3)$.

2.3. Experimental details

A stack of NIKF1-BR2 emulsion plates was exposed to the ^{12}C beam at 4.5 A GeV/c in the high-energy Institute JINR (Dubna, Russia) Each plate was scanned through, "along-the-track", using a Leitz Ortholux microscope with the optics 100× objective and 20× occular. The events within 20 μm thickness from the top or bottom surface of the plates were not analysed. The grey tracks were identified by their grain density g as $0.6g^0 < g < 1.4g^0$, where g^0 is the plateau grain density for singly charged particles of a range greater than 3mm. The selection of target proton tracks was done according to the work of Breivik et al. [14]. Only those grey tracks were selected for the analysis that did not show any signs of interaction or decay at their end points. This was done to eliminate the gray tracks which were not due to the target protons. Care was taken so that no contamination takes place betwen the pions and protons emitted as projectile fragments. Relativistic protons emitted within the projectile fragmentation region were selected by the method of angular cut [15] at an angle of θ given by

$$\Theta = \frac{0.2}{E_{lab}(\mathrm{GeV})}.$$

In this way, 5250 gray tracks have been identified. The emission angles of black (b), grey (g) and shower (s) track particles for both "hot" and "cold" group of events were measured as described in Ref. 6.

3. Separation of "hot" and "cold" events

Events with the two different temperature, i.e. the "hot" and "cold" classification, was made in accordance with the work of Baumgardt et al. [17]. The transverse momentum of α-particles emitted as projectile fragments, were calculated from the relation

$$P_T = Am_0 \frac{v}{\sqrt{1-\beta^2}} \sin\theta,$$

where A is the atomic number, m_0 is the nucleon rest mass, v is the α-particle velocity, $1/\sqrt{1-\beta^2}$ is the Lorentz factor of the projectile fragment and θ is the laboratory-frame angle to the incoming beam direction. Assuming the momentum distribution (P_T) to be the Maxwell-Boltzmann distribution in the projectile rest frame at a temperature T, the integral frequency distribution of the P_T per nucleon squared, $Q = (P_T/A)^2$ is

$$\ln F(>Q) = -\frac{A}{2m_0 T} Q.$$

Since this relation is linear, one can easily verify the agreement of a set of data to the Maxwell-Boltzmann distribution. A cumulative plot of $\ln F(>Q)$ as a function of Q shows a non-linear distribution. It was interpreted as a mixture of two Maxwell-Boltzmann components with two distinctly different temperatures: one "hot" and the other "cold". A minimum chi-square fit yielded 40 MeV and 10 MeV for the two temperatures, respectively. It

was observed that nearly 60 % of the events belong to the "cold" group and about 40 % to the "hot" group, the details of which are discussed in Ref. 8.

4. Monte-Carlo Simulation

In studies of correlation functions, pseudo-correlations arise from the broad mutiplicity (n) distribution and the dependence of one-particle spectrum on the multiplicity, as well as the trivial correlations due to kinematical constraints in the individual events.

The simulation was based on the following assumptions:

(i) particles of all types are independent of each other,

(ii) the multiplicity distribution in each ensemble of Monte-Carlo events reproduces the empirical multiplicity spectrum of the real ensemble;

(iii) the angular distribution of all types of particles coincides with the empirical 'semi-inclusive' (i.e, at fixed n_a, n_b and n_g) angular distribution.

Because of the lack of precise knowledge of the energy and momentum of the system, we have used a random sampling method on the corresponding experimental distribution to generate Monte-Carlo events. This method has been successfully applied for hadron-nucleus [18] and nucleus-nucleus [19,16,7] interactions. Gulamov et al. [20] have compared correlation functions (C) calculated from the inclusive ensembles of random events generated according to the method adopted here, i.e., the independent emission model (IEM), with the correlation function generated according to the cylindrical phase-space model (CPSM) (which gives the contribution of correlation due to kinematics). They observed that conservation laws led to an increase of the long-range and a decrease of the short-range correlations. Therefore, any observation of an excess of short-range correlation over the predictions of the IEM indicates the presence of a dynamical effect that cannot be explained by the conservation laws. Moreover, the difference between the experimental results and the model predictions increase if we use the conservation laws derived from the statistical theory of multiple production.

By comparing the normalised correlation function R obtained from experiment with R_M obtained from Monte-Carlo simulated events, one can search for the dynamical contribution to the correlation. The difference $R_D = R - R_M$ (dynamical surplus) can be interpreted as a manifestation of dynamical correlation.

5. Results and discussion

We calculate the two-particle correlation function with the help of Eq. (1) for all events. Fig. 1a and b show the normalised two-particle correlation function along with the Monte-Carlo simulated values for "cold" events and "hot" events, respectively. The curves in the figures represent the values of the correlation functions given by the Monte-Carlo calculations and the circles represent the experimental values. The figures functions

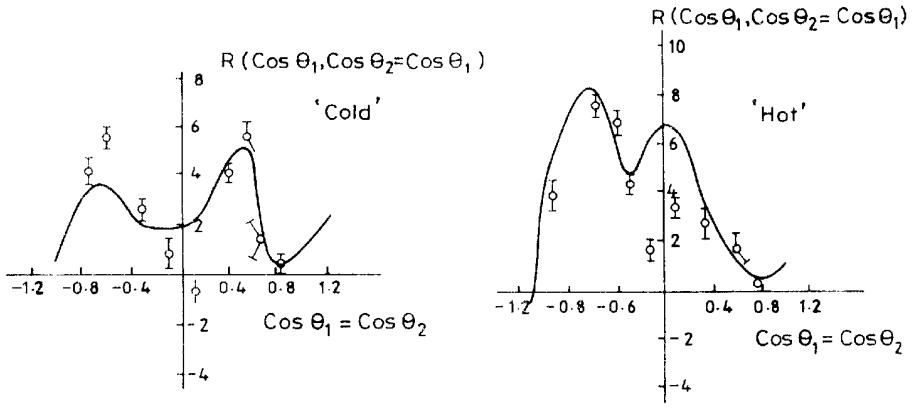

Fig. 1. The normalised two particle correlation function for different values of $\cos\theta$*: a) for "cold" and b) for "hot" events. The curves show the Monte-Carlo simulated values.*

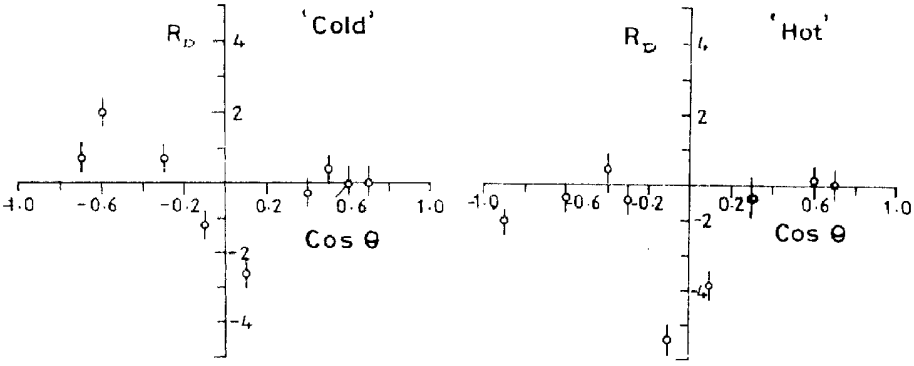

Fig. 2. The dynamical surplus (excess) correlation over the Monte-Carlo background for a) "cold" events and b) for "hot" events.

giving an idea of the magnitude of the short-range two-particle correlation among protons for different values of $\cos\theta$. One observes statistically significant excess correlation over the Monte-Carlo background in both "cold" and "hot" events. In the case of "cold" events, the correlation is extremely prominent at the angles between 85° and 95° and at about 125°, whereas in the case of "hot" events, the correlation occurs only from 85° to 90°. The dynamical surplus, i.e., the excess correlation over Monte-Carlo background is shown in Figs. 2a and b. The errors shown are only statistical [21] (the details are given in the Appendix).

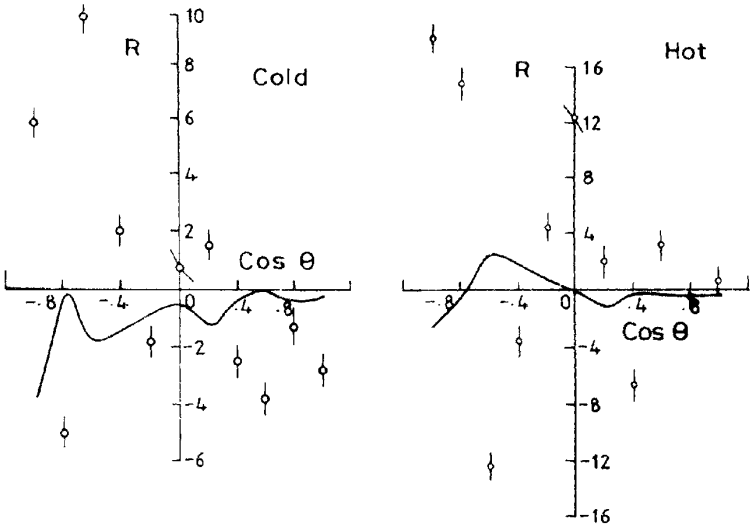

Fig. 3. The normalised three-particle correlation function for different values of $\cos\theta$*: a) for "cold" events and b) for "hot" events. The curves show the Monte-Carlo simulated values.*

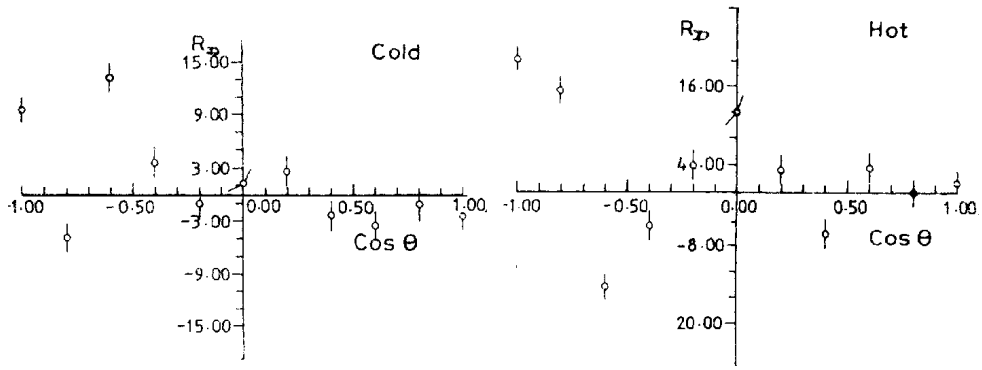

Figure 4. The dynamical surplus (excess) correlation over the Monte-Carlo background a) for "cold" events and b) for "hot" events.

Similar plots for three-particle correlations are shown in Figs. 3a and b. The corresponding dynamical surplus is depicted in Figs. 4a and b. In this case, the correlation exists over the backward hemisphere for "hot" events. The maximum occurs at about 180°. "Cold" events also show correlation in the backward hemisphere - the maximum is at about 130°.

6. Conclusion

Correlated protons are emitted preferentially in the backward hemisphere for both "hot" and "cold" events. This may be interpreted as the so called "side splash" effect, and region of the occurrence depends on whether the events belong to "hot" or "cold" group. This analysis provides new data on "hot" and "cold" events produced by interaction of ^{12}C at 4.5. A GeV/c in AgBr.

Acknowledgements

Authors would like to thank professor K. D. Tolstov, JINR, Russia, for providing the exposed and developed emulsion plates. We also greatfully acknowledge the financial help given by the University Grant Commission (Govt. of India) under their COSIST programme.

Appendix

The calculation of errors. From the experimental data, the two-particle correlation function is calculated as

$$\begin{aligned} R(\cos\theta_1,\cos\theta_2) &= < n_1 n_2 > / [< n_1 >< n_2 >] - 1, \quad \text{for} \cos\theta_1 \neq \cos\theta_2 \\ &= < n(n-1) > / < n^2 > -1, \qquad \text{for} \cos\theta_1 = \cos\theta_2, \end{aligned}$$

where n_1 and n_2 are the black multiplicities in a small interval of $\delta(\cos\theta)$ around $\cos\theta_1$ and $\cos\theta_2$. The variance of R is given by

$$\begin{aligned} V[R] = {} & \{< n_1 >^2 < n_2 >^2 < n_1 n_2 >^2 - 2 < n_1^2 n_2 >< n_1 n_2 >< n_1 >< n_2 >^2 \\ & -2 < n_1 n_2^2 >< n_1 >^2 < n_2 >< n_1 n_2 > + < n_1^2 >< n_1 n_2 >^2 < n_2 >^2 \\ & + < n_2^2 >< n_1 n_2 >^2 < n_1 >^2 + 2 < n_1 n_2 >^3 < n_1 >< n_2 > \\ & - < n_1 n_2 >^2 < n_1 >^2 < n_2 >^2 \} [N < n_1 >^4 < n_2 >^4]^{-1} \\ & + O(1/N^2) \qquad \text{for} \quad \cos\theta_1 \neq \cos\theta_2, \end{aligned}$$

and

$$\begin{aligned} V[R] = {} & \{< n^4 >< n >^2 - 4 < n^3 >< n^2 >< n > + 4 < n^2 >^3 \\ & - < n^2 >^2 < n >^2 + 2 < n^2 >< n >^2 - 4 < n^2 >^2 < n > \\ & + 2 < n^2 >< n >^3 + < n^2 >< n >^2 - < n >^4 \} [N < n >^6]^{-1} \\ & + O(1/N^2) \qquad \text{for} \quad \cos\theta_1 = \cos\theta_2. \end{aligned}$$

N is the tolal number of inelastic events, $O(1/N^2)$ is a polynomial which is negligible when calculating the errors, in comparison with the other terms. Similarly, the three-particle

correlation function is experimentally obtained as

$$R(\cos\theta_1, \cos\theta_2, \cos\theta_3)$$
$$= < n(n-1)(n-2) > / < n >^3 - 3 < n(n-1) > / < n >^2 + 2$$
$$\text{for} \quad \cos\theta_1 = \cos\theta_2 = \cos\theta_3.$$

The variance of this quantity is calculated term by term and instead of giving the long algebraic expression of the net variance, we have computed it and shown the corresponding errors in the figures.

References

1) B. Nilsson-A. Lmquist and E. Stenlund, Comp. Phys. Comm. **43** (1987) 387; S. Wang et al., Phys. Rev. **C 44** (1991) 1091; J. Barrette et al., (E814 Collaboration), Phys. Rev **C 46** (1992) 312 (20Si+Al(Pb) at 14.6 GeV/c; J. Jiang et al., Phys. Rev. Lett. **68** (1992) 2739; Nu. Xu. - (E814 Collaboration), Nuclear Phys. **A553** (1993) 785c; H. Fuchs and K. Mohring, Rep. Prog. Phys. **3** (1994) 231; E. Stenlund (EMUO1 Collaboration), Nucl. Phys. **A 590** (1995) 597c; L. Martin et al., Nucl. Phys. **A 583** (1995) 407;
2) M. I. Adamovich et al., Phys. Lett. **B 262** (1991) 369;
3) E. Sterlund and I. Otterlund, Nucl. Phys. **B 198** (1982) 407;
4) B. Anderson, S. I. A. Garpman, G. Nitsson, I. Otterlund and K. B. Bhalla, Nucl. Phys. **B 191** (1981) 173;
5) A. Jurak and A. Linscheid, Acta Physica Polonica **B 66** (1977) 875;
6) G. Giacomelli and M. Jacob, Phys. Peps. **55** (1979) 1;
7) Gustafsson et. al., Phys. Rev. Letters **53** (1984) 544; D. Ghosh, J. Roy and R. Sengupta, Z. Phys. **A 327** (1987) 233;
8) D. Ghosh, J. Roy and R. Sengupta, J. Phys. G: Nucl. Phys. **14** (1988) 711;
9) D. Ghosh, J. Roy, R. Sengupta and S. Sarkar, J. Phys. G: Nucl. Phys. **18** (1992) 935;
10) D. Ghosh, A. Deb, R. Sengupta, S. Das and K. Purkait, J. Phys. G: Nucl. Phys. **19** (1993) L19;
11) D. Ghosh, R. Sengupta and S. Sarkar, Hadronic Journal **12** (1989) 279;
12) D. Ghosh, J. Raya, R. Sengupta and S. Sarkar, Z. Phys. **A 342** (1992) 191;
13) E. M. Levin, M. G. Ryskin and N. N. Nikolaev, Z. Phys. **C 5** (1980) 285;
14) F. O. Breivik, T. Jacobsen and S. O. Sorensen, Phys. Scr. **30** (1984) 392;
15) M. I. Adamovich et al. (EMU01), Phys. Lett. B223 (1989) 262;
16) D. Ghosh, J. Roy and R. Sengupta, Nucl. Phys. **A 468** (1987) 719;
17) H. G. Baumgardt, E. M. Friedlander and E. Schopper, J. Phys. G: Nucl. Phys. **7** (1981) L175;
18) D. Ghosh, J. Roy, K. Sengupta, M. Bsu, A Ghattacharya, T. Guhathakurta and S. Naha, Phys. Rev. **D 26** (1982) 2983;
19) G. M. Chernov, K. G. Gulamov, U. Gulyamov, S. G. Nasyrov and . N. Srechnikova, Nucl. Phys. **A 280** (1980) 478;
20) K. G. Gulamov, S. A. Azimov, A. I. Bondarenko, V. I. Petrov, R. V. Buzimatov and N. S. Scripnik, Z. Phys. **A 280** (1977) 107;

21) W. Bell et al., Z. Phys. **C 22** (1984) 109.

DINAMIČKE KORELACIJE MEĐU PROTONIMA SREDNJIH ENERGIJA U ”VRUĆIM” I ”HLADNIM” RELATIVISTIČKIM TEŠKO-IONSKIM SUDARIMA

Proučavaju se dvo- i tročestične dinamičke korelacije, posebno za ”vruće” i za ”hladne” procese u sudarima ^{12}C-AgBr pri 4,5 A GeV/c.